

Sculpting Efficiency: Pruning Medical Imaging Models for On-Device Inference

Sudarshan Sreeram

Bernhard Kainz

Department of Computing, Imperial College London, London, United Kingdom

{sudarshan.sreeram19, b.kainz}@imperial.ac.uk

<https://biomedia.doc.ic.ac.uk/>

Abstract

Applying ML advancements to healthcare can improve patient outcomes. However, the sheer operational complexity of ML models, combined with legacy hardware and multi-modal gigapixel images, poses a severe deployment limitation for real-time, on-device inference. We consider filter pruning as a solution, exploring segmentation models in cardiology and ophthalmology. Our preliminary results show a compression rate of up to **1148x** with minimal loss in quality, stressing the need to consider task complexity and architectural details when using off-the-shelf models. At high compression rates, filter-pruned models exhibit faster inference on a CPU than the GPU baseline. We also demonstrate that such models' robustness and generalisability characteristics exceed that of the baseline and weight-pruned counterparts. We uncover intriguing questions and take a step towards realising cost-effective disease diagnosis, monitoring, and preventive solutions.

1. Introduction

CNNs thrive in multi-disciplinary settings, but their architectural depth correlates with rapid growth in their footprint and operational expenses [10]. Despite the impressive range of such models in academic healthcare research, they remain rare in clinical practice [7] due to this scale-related complexity that poses challenges for effective deployment.

For instance, models in point-of-care (POC) systems and those in the daily routine for assessing medical images must maintain clinical utility while being performant in compute-limited settings. This deployment limitation is apparent given that healthcare institutions seldom prioritise upgrading their IT infrastructure [22]. Furthermore, certain imaging modalities produce gigapixel images, often exceeding 100K pixels in each dimension [21]; large models operating on such images place hardware constraints that existing infrastructure cannot support. Shifting tasks to cloud services can jeopardise the confidentiality of patient data, and investing in advanced hardware may not be feasible for hospitals

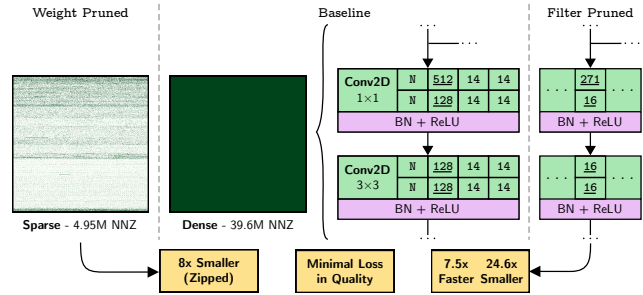


Figure 1: Visualisation of weight and filter pruning paths. The two layers are from a bottleneck block in DeepLabV3. *Left:* Parameter sparsity diagrams, where zeroed weights are coloured white; the baseline is globally weight-pruned to 87.5% sparsity. *Right:* Channel count difference for an 87.5% filter-pruned model (1.76M params.); the layer structure remains intact, making the model deep and lean.

with limited funds. An optimal solution permits healthcare specialists to perform intricate image analysis on various platforms, from smartphones to web browsers in hospital computers, ensuring widespread utility and data protection.

Model compression, specifically pruning, is a promising option; it addresses maintaining a model's predictive power while minimising resource usage. Pruning is an umbrella term for a broad set of methods that remove redundant network weights [24]. It is crucial in enabling the exciting prospect of inferencing directly on portable and tabletop instruments or even smartphones connected to medical-grade scanners like POCUS ultrasound devices, allowing clinics to make the most out of their existing setup while maintaining patient data within its bounds.

ML-augmented POC devices are cost-effective for asymptomatic patients in tackling abnormalities by aggregating quantitative metrics that indicate disease progression and signal early treatment measures [16, 13]. For instance, cardiomyopathy and diabetic retinopathy are widespread chronic diseases [11, 19] that pose dire consequences if left untreated; they typically cause irreversible damage and re-

quire exorbitantly expensive treatments [5]. Automated detection is crucial for the early diagnosis of both conditions.

For healthcare specialists, ML-based workflows facilitate rapid evaluation and measurement precision; human assessment is laborious and shows inter-observer variability despite decades of training. Such workflows ease the burden of backlogged cases when well-trained specialists are scarce [5]. The intention is not to replace specialists’ expertise but to accelerate and foster evidence- and analysis-backed decisions [4], allowing them to focus on critical aspects of patient care, such as treatment planning.

Medical instruments are similar to entertainment devices in that they capture and post-process information at high throughput with limited compute capacity for heavy ML workloads. Optimising for such devices offers reduced latency – crucial for time-sensitive emergencies – and better reliability by eliminating the need for internet access.

We only found limited research on model compression in healthcare domains; they primarily focus on NAS methods [23] and knowledge distillation [14] rather than pruning. A few recent works discuss pruning in efficiently identifying COVID-19 lung lesions [1, 15], but they approach the problem from a healthcare-first perspective, focusing on clinical utility as a misdiagnosis can be detrimental to patient health. We take an ML-first approach to realise practical feasibility while scrutinising boilerplate practices. In this paper, we uncover inefficiencies resulting from researchers’ oversight in configuring off-the-shelf models for the specific needs of their studies and identify intriguing avenues to explore.

2. Method

A core barrier to using medical imaging models on limited hardware is that large activations rapidly deplete memory, especially with gigapixel inputs [21]. Some opt for patch-wise processing as downsampling may be too lossy, and while such workarounds can be effective, they fail to address the limitation’s source: *the underlying architecture*. Clinical researchers often follow a data-driven approach [22], picking off-the-shelf models for solutions. We hypothesise that this approach may cause deep-rooted flaws, hindering the prospect of use on medical instruments.

Weight Pruning: We use two unstructured L1-norm weight pruning strategies to sparsify models; one is locally scoped and allocates the sparsity budget per layer, while the other is globally scoped and distributes it across all prunable layers. While sparse tensors yield a storage benefit, most runtime libraries and general-purpose hardware cannot accelerate sparse matrices’ computation due to high irregularity [20, 9], as in Figure 1. As the pruned weights exist in memory, pruned models perform no better than the baseline and exhibit the same *footprint metrics* (e.g., latency, MACs, size). We do not consider accelerators and only see weight-pruning as a tool to reveal immediate redundancies.

Filter Pruning: With a locally-scoped structured L1-norm filter (or channel) pruning strategy, we create deep, dense, and lean networks [9]. Reducing channels results in fewer activation maps at runtime, and the high regularity enables the model to run on standard hardware [8]. These pruned models retain architectural similarity to the baseline, differing only in channel counts, as in Figure 1.

3. Experiments

Our work revolves around DeepLabV3-based segmentation models. This model (39.6M params.) uses a ResNet-50 backbone and leverages atrous convolutions via the atrous spatial pyramidal pooling (ASPP) module to extract multi-scale contextual information while preserving spatial resolution [3]. With both pruning methods, we adopt a one-shot schedule and fine-tune the model for 5~10 epochs. In each pruning run, we set the target (sparsity/fraction of filters) as:

$$\text{target} = 1 - \text{pow}(0.5, \frac{x}{\text{Run index in an experiment group}})$$

The curve incrementally increases the target, slowing down with each run. A high target can severely corrupt a model’s predictive power to the point of no return. To assess model performance, especially for filter-pruned models, we run inference on both the CPU and GPU using the Intel i5 13600K (64 GB RAM) and an Nvidia RTX 4080 (16GB).

3.1. Cardiac Ultrasound

The EchoNet-Dynamic dataset [12] comprises 10K+ cardiac ultrasound videos with a resolution of 112×112 . The segmentation target is the left ventricle, a heart chamber, and the trend in its volume over time correlates with prognosis [13]. For frame-level segmentation, the dataset curators proposed a DeepLabV3-based model (158.76 MB) with roughly 7.8 GMACs. Our baseline reproduction achieves a DICE score of 0.9098 ± 0.0026 and 0.9334 ± 0.0017 on the systolic and diastolic frames. It has a latency / throughput of 31.82 ms / 31 FPS on a CPU and 5.279 ms / 189 FPS on a GPU; we use a scripted PyTorch model under the inference context mode. Notably, the mean sampling rate of videos is 51 FPS, so CPU inference is unsuitable for real-time use.

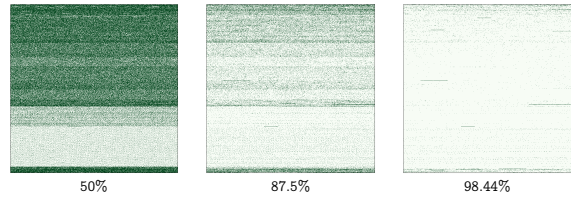


Figure 2: Parameter sparsity diagrams for globally-scoped weight pruned models; non-zero values are coloured green.

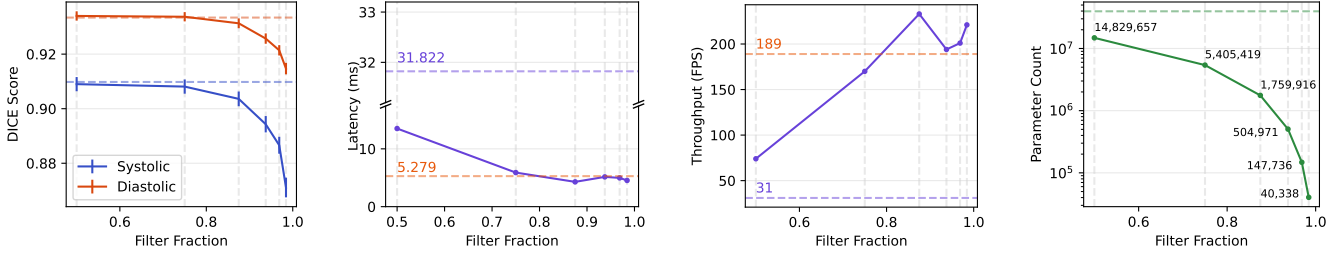


Figure 3: Quality and performance characteristics for all six filter pruning runs. *Left*: Trend in DICE scores of systolic and diastolic frames with compression rate. *Middle*: Latency and throughput trends; the dotted orange and violet markers represent the GPU and CPU baselines, respectively. *Right*: Decline in number of model parameters with compression rate.

As in Figure 4, globally weight-pruned models show impeccable resiliency to high sparsity, while a uniform, local strategy hurts model quality and fails at such high targets [2]; some layers have more redundancy than others. Figure 2 highlights that even at 98.4% sparsity (633K NNZ params.), the quality remains within 1% of the baseline, evincing that DeepLabV3 is remarkably oversized for this task. Our filter pruning results concur. In Figure 3, the extreme case (0.984) achieves DICE scores within 4% of the baseline while being 1148x smaller (34.5K params.). Moreover, the best case (0.875) is within 0.7% of the baseline, and its throughput is 7.5x higher at 233 FPS, making it viable for real-time use. This model is just as fast on a CPU as the GPU baseline, a striking improvement that results solely from pruning. The unexpected performance shift, likely due to memory access patterns or the limits of parallelising small workloads, warrants a closer look.

Using an off-the-shelf model without considering task complexity is akin to using a truck to transport a grape. DeepLabV3 can, as proposed, handle 20 segmentation classes, but ours is a binary problem. The parameter sparsity diagram in Figure 2, specifically the 50% one, indicates the immediate redundancy. The missing band belongs to the ASPP module, precisely three atrous convolutions (each 4.71M params.), forming 35.7% of the model.

Atrous convolutions are effective in the presence of scale-affecting transforms (e.g., varying imaging parameters) and when the feature map size is smaller than the atrous rate. Here, the backbone encoded feature map has a resolution of 14×14 , but the ASPP module is configured with atrous rates 12, 24 and 36; all three convolutions reduce to pointwise ones [3]. The minimum input size to circumvent this is 288×288 , more than twice the frame size. Also, the videos do not usually differ in scale as trained sonographers obtain them; the influence of patient anatomy is marginal. The oversight in conforming to these conditions, among others in medical imaging research, has baked in notable redundancy, enabling extreme compression rates.

ters) and when the feature map size is smaller than the atrous rate. Here, the backbone encoded feature map has a resolution of 14×14 , but the ASPP module is configured with atrous rates 12, 24 and 36; all three convolutions reduce to pointwise ones [3]. The minimum input size to circumvent this is 288×288 , more than twice the frame size. Also, the videos do not usually differ in scale as trained sonographers obtain them; the influence of patient anatomy is marginal. The oversight in conforming to these conditions, among others in medical imaging research, has baked in notable redundancy, enabling extreme compression rates.

3.2. Fundus Retina Scans

A follow-up question we sought to address from the first study is whether a filter pruning approach would scale well to tasks requiring fine, intricate segmentations; the EchoNet task is quite simple as the target is a single, smooth and continuous blob in roughly the same position for every sample, as in Figure 5. We use a pre-processed version of the FIVES dataset formed of fundus photographs with a resolution of 1024×1024 [6, 5], larger than the minimum for DeepLabV3. The encoded feature map size is 128×128 . While segmenting the vasculature is still a binary problem and continuous, the vessels vary in shape and size. As images of the left and right eye are flipped, the model must adapt to variations in the orientation of the overall vasculature and the vessels themselves.

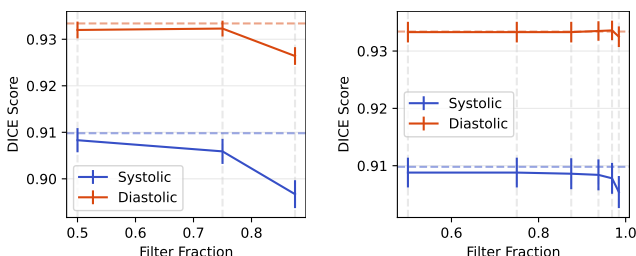


Figure 4: Quality trends of locally (*left*) and globally (*right*) weight pruned models. The dotted line is the baseline.

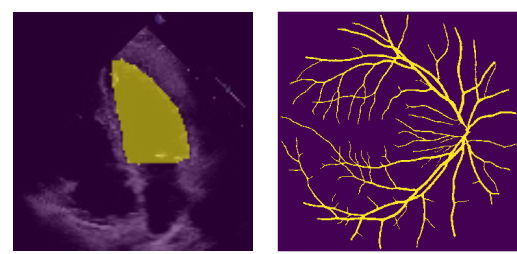


Figure 5: Sample diastolic frame segmentation (*left*) vs retinal vasculature segmentation (*right*).

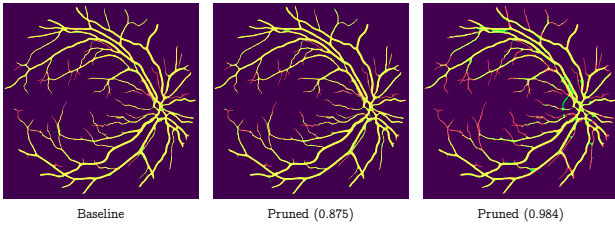


Figure 6: Difference images with respect to the ground truth for segmentations from the baseline and pruned models. *Red*: Missing in predictions but present in ground truth. *Green*: Present in predictions but missing in ground truth.

ture, arguably making the task much harder than before.

Our baseline achieves a DICE score of 0.8582 ± 0.0118 . Each sample, now $83.55x$ larger, occupies 12 MB, resulting in 654.25 GMACs due to sizeable activations, 93x higher than before. Thus, the model has a latency / throughput of 2329.625 ms / 0 FPS on a CPU and 60.49 ms / 17 FPS on a GPU. Fundus cameras are vital in combating the cause of preventable blindness, especially in underserved regions, so efficiency is crucial, even if real-time use is optional.

The quality trends are largely similar, albeit with a larger drop at high filter fractions. The best case (0.875) is 22.5x smaller (1.75M params.) and within 3% of the baseline. Unlike before, the CPU performance is monotonic, with this model having a latency / throughput of 234.73 ms / 4 FPS, nearly 10x faster than the baseline. Figure 6 reveals the integrity of its prediction with a noteworthy observation: fine details vanish as more filters are removed. This is clearly visible in the 0.984 case, achieving 66 FPS on a CPU, beating the GPU baseline. A practitioner can overcome the quality trade-off with post-processing (e.g., extracting key point descriptors). While we meet the necessary conditions, the ASPP module still remains largely redundant. The excess capacity for accommodating 20 classes is likely a dominant factor, but we defer further exploration. Extending the baseline training to reach higher quality may also provide a better starting point for pruning.

4. AI Safety

Robustness is a critical ethical consideration, as model predictions can impact patient outcomes. We test the robustness of our EchoNet models, specifically the 87.5% sparse weight-pruned and 0.875 filter-pruned ones, to noise. Figure 7 evinces that the filter-pruned model excels in preserving segmentations despite higher noise ratios, better than both the baseline and weight-pruned counterparts. A similar trend, not visualised, emerges for the diastolic frame. Thus, even with specialised solutions to accelerate weight-pruned models, filter-pruned models are inherently better.

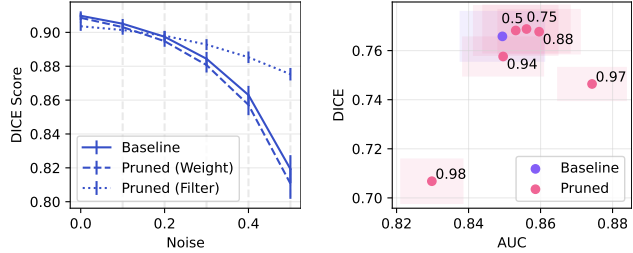


Figure 7: *Left*: Robustness of the baseline, weight-pruned and filter-pruned models to noise on the systolic frames. *Right*: Generalisability of filter-pruned models trained on FIVES to an out-of-distribution dataset (DRIVE).

Generalisability to out-of-distribution data is another critical consideration. Often, the data used to train models do not capture the diversity of real-world data due to different scanner types and varying patient physiology. We test our FIVES filter-pruned models on the DRIVE dataset [18]. Our results, as in Figure 7, show that filter-pruned models generalise better up to a point.

5. Conclusion

We motivate and investigate CNN model pruning in medical imaging to make previously inefficient models practically deployable. Our initial work narrows down on the cause of deep-rooted inefficiencies via two case studies. The EchoNet study sets up the context to showcase the severity of such inefficiencies, and the FIVES study considers nonconformity to implicit architectural constraints and low task complexity as possible causes of redundancy. In both cases, the underlying architecture’s excess capacity facilitates extreme compression rates, attributing our hypothesis. However, we acknowledge ample prospects for future work in refining this hypothesis.

As filter pruning is local, one can opt to train, from scratch, a model naively pruned to an apt capacity, avoiding an expensive baseline. This is a promising next step as it saves considerable time for practitioners on a limited training budget. We are eager to delve into multi-class and multi-label segmentation tasks, crucial in healthcare domains such as histopathology, to continue our review of the ASPP module. Replacing it with a smaller, custom segmentation head may fare better for both model quality and performance. We also see value in sensitivity analysis and hardware-aware heuristics contributing to more informed pruning decisions [17]. Other exciting avenues include collaborating with clinicians to assess utility, using layer-specific pruning strategies, chaining optimisations together such as sparsity-aware quantisation-aware training, and exploring alternate network architectures designed explicitly for efficiency-critical use cases.

References

[1] Mohit Agarwal, Sushant Agarwal, Luca Saba, Gian Luca Chabert, Suneet Gupta, Alessandro Carriero, Alessio Pasche, Pietro Danna, Armin Mehmedovic, and Gavino Faa et al. Eight pruning deep learning models for low storage and high-speed COVID-19 computed tomography lung segmentation and heatmap-based lesion localization: A multicenter study using COVLIAS 2.0. *Computers in Biology and Medicine*, 146:105571, July 2022. [2](#)

[2] Davis Blalock, Jose Javier Gonzalez Ortiz, Jonathan Franckle, and John Guttag. What is the state of neural network pruning?, 2020. [3](#)

[3] Liang-Chieh Chen, George Papandreou, Florian Schroff, and Hartwig Adam. Rethinking atrous convolution for semantic image segmentation, 2017. [2, 3](#)

[4] Katharine E. Henry, Rachel Kornfield, Anirudh Sridharan, Robert C. Linton, Catherine Groh, Tony Wang, Albert Wu, Bilge Mutlu, and Suchi Saria. Human-machine teaming is key to AI adoption: clinicians' experiences with a deployed machine learning system. *npj Digital Medicine*, 5(1), July 2022. [2](#)

[5] Benjamin Hou. Domain agnostic pipeline for retina vessel segmentation, 2023. [2, 3](#)

[6] Kai Jin, Xingru Huang, Jingxing Zhou, Yunxiang Li, Yan Yan, Yibao Sun, Qianni Zhang, Yaqi Wang, and Juan Ye. FIVES: A fundus image dataset for artificial intelligence based vessel segmentation. *Scientific Data*, 9(1), Aug. 2022. [3](#)

[7] Christopher J. Kelly, Alan Karthikesalingam, Mustafa Suleyman, Greg Corrado, and Dominic King. Key challenges for delivering clinical impact with artificial intelligence. *BMC Medicine*, 17(1), Oct. 2019. [1](#)

[8] Zhuang Liu, Mingjie Sun, Tinghui Zhou, Gao Huang, and Trevor Darrell. Rethinking the value of network pruning, 2019. [2](#)

[9] Huizi Mao, Song Han, Jeff Pool, Wenshuo Li, Xingyu Liu, Yu Wang, and William J. Dally. Exploring the regularity of sparse structure in convolutional neural networks, 2017. [2](#)

[10] Gaurav Menghani. Efficient deep learning: A survey on making deep learning models smaller, faster, and better, 2021. [1](#)

[11] World Health Organisation. Cardiovascular diseases — who.int. https://www.who.int/health-topics/cardiovascular-diseases#tab=tab_1. [Accessed 18-Jun-2023]. [1](#)

[12] David Ouyang, Bryan He, Amirata Ghorbani, Matthew P. Lungren, Euan A. Ashley, David H. Liang, and James Y. Zou. Echonet-dynamic: a large new cardiac motion video data resource for medical machine learning, 2019. [2](#)

[13] David Ouyang, Bryan He, Amirata Ghorbani, Neal Yuan, Joseph E. Ebinger, C. Langlotz, Paul A. Heidenreich, Robert A. Harrington, David H. Liang, Euan A. Ashley, and James Y. Zou. Video-based ai for beat-to-beat assessment of cardiac function. *Nature*, 580:252–256, 2020. [1, 2](#)

[14] Dian Qin, Jia-Jun Bu, Zhe Liu, Xin Shen, Sheng Zhou, Jing-Jun Gu, Zhi-Hua Wang, Lei Wu, and Hui-Fen Dai. Efficient medical image segmentation based on knowledge distillation. *IEEE Transactions on Medical Imaging*, 40(12):3820–3831, 2021. [2](#)

[15] Sivaramakrishnan Rajaraman, Jenifer Siegelman, Philip O. Alderson, Lucas S. Folio, Les R. Folio, and Sameer K. Antani. Iteratively pruned deep learning ensembles for COVID-19 detection in chest x-rays. *IEEE Access*, 8:115041–115050, 2020. [2](#)

[16] Bailey Y. Shen and Shizuo Mukai. A portable, inexpensive, nonmydriatic fundus camera based on the raspberry pi® computer. *Journal of Ophthalmology*, 2017:1–5, 2017. [1](#)

[17] Maying Shen, Hongxu Yin, Pavlo Molchanov, Lei Mao, Jianna Liu, and Jose M. Alvarez. Halp: Hardware-aware latency pruning, 2021. [4](#)

[18] J. Staal, M.D. Abramoff, M. Niemeijer, M.A. Viergever, and B. van Ginneken. Ridge-based vessel segmentation in color images of the retina. *IEEE Transactions on Medical Imaging*, 23(4):501–509, 2004. [4](#)

[19] Jaimie D Steinmetz, Rupert R A Bourne, Paul Svitil Brant, Seth R Flaxman, Hugh R B Taylor, Jost B Jonas, Amir Aberhe Abdoli, Woldu Aberhe Abrha, Ahmed Abualhasan, and Eman Girum Abu-Gharbieh et al. Causes of blindness and vision impairment in 2020 and trends over 30 years, and prevalence of avoidable blindness in relation to VISION 2020: the right to sight: an analysis for the global burden of disease study. *The Lancet Global Health*, 9(2):e144–e160, Feb. 2021. [1](#)

[20] Ziheng Wang. Sparsednn: Fast sparse deep learning inference on cpus, 2021. [2](#)

[21] Yan Xu, Zhipeng Jia, Liang-Bo Wang, Yuqing Ai, Fang Zhang, Maode Lai, and Eric I-Chao Chang. Large scale tissue histopathology image classification, segmentation, and visualization via deep convolutional activation features. *BMC Bioinformatics*, 18(1), May 2017. [1, 2](#)

[22] Angela Zhang, Lei Xing, James Zou, and Joseph C. Wu. Shifting machine learning for healthcare from development to deployment and from models to data. *Nature Biomedical Engineering*, 6(12):1330–1345, July 2022. [1, 2](#)

[23] Zhong Zheng and Guixia Kang. Model compression with nas and knowledge distillation for medical image segmentation. In *2021 4th International Conference on Data Science and Information Technology*, DSIT 2021, page 173–176, New York, NY, USA, 2021. Association for Computing Machinery. [2](#)

[24] Michael Zhu and Suyog Gupta. To prune, or not to prune: exploring the efficacy of pruning for model compression, 2017. [1](#)